Transition probabilities in ^{154}Gd: Evidence for X(5) critical point symmetry

D. Tonev,[1,*] A. Dewald,[1] T. Klug,[1] P. Petkov,[1,2] J. Jolie,[1] A. Fitzler,[1] O. Möller,[1]
S. Heinze,[1] P. von Brentano,[1] and R. F. Casten[3]
[1]*Institut für Kernphysik der Universität zu Köln, D-50937 Köln, Germany*
[2]*Bulgarian Academy of Sciences, Institute for Nuclear Research and Nuclear Energy, 1784 Sofia, Bulgaria*
[3]*WNSL, Yale University, New Haven, Connecticut 06520-8124, USA*
(Received 7 November 2003; published 29 March 2004)

Lifetime measurements in ^{154}Gd were performed by means of the recoil distance Doppler-shift method. Excited states of ^{154}Gd were populated via Coulomb excitation with a ^{32}S beam at 110 MeV delivered by the FN tandem accelerator of the University of Cologne. The determined transition probabilities as well as the low-spin level scheme of ^{154}Gd demonstrate a good agreement with the predictions of the critical point symmetry X(5). Comparison of specific experimental observables for the $N=90$ rare earth isotones with the calculations of the X(5) model clearly show that ^{154}Gd is one of the good examples of the realization of the X(5) dynamical symmetry. In addition, the experimental data are compared to fits in the framework of the IBA and the general collective model.

DOI: 10.1103/PhysRevC.69.034334 PACS number(s): 21.60.Fw, 21.10.Re, 21.10.Tg, 23.20.−g

I. INTRODUCTION

Phase transitions in physics lead to very interesting phenomena and represent an appealing challenge for a detailed investigation, both experimentally and theoretically. Nuclei as dynamic systems can undergo phase transitions associated with a change of the shape of their equilibrium configuration. In the works of Iachello [1,2], it was shown that new dynamical symmetries can describe atomic nuclei at the critical points of phase transitions from spherical to deformed shapes. The new symmetries, called E(5) and X(5), are obtained within the framework of the collective model [3] under some simplifying approximations. It is known that geometrically the nucleus can be described by three Euler angles defining the orientation of the body-fixed coordinate system in space, and by the quadrupole deformation parameters β and γ [3]. The nuclear potential in the X(5) case, which describes the nucleus at the critical point of the U(5)-SU(3) phase transition (spherical to prolate axial deformation), is approximated by a square well and a harmonic oscillator potential with respect to the β and γ degrees of freedom, respectively. In the case of the E(5) critical point symmetry (phase transition from spherical to deformed γ-unstable nucleus), the potential is flat in the γ direction. In addition, in both cases the β and γ degrees of freedom are considered to be decoupled. These potentials allow for analytical solutions of the eigenfunction problem, leading to closed expressions for the energies of the excited states and the transition rates.

The target of our investigation is the nucleus ^{154}Gd, which is expected to be one of the very promising candidates for X(5) critical point symmetry. This fact is illustrated in Fig. 1, where characteristic energy ratios in some $N=90$ isotones are compared to the values predicted in the framework of X(5). Many theoretical and experimental efforts have already been dedicated to the study of that appealing nucleus which is rich in interesting phenomena (cf., e.g., Refs. [4–8], and references therein). The most recent investigation [9], for instance, infers a new coexisting weakly deformed structure based on the 0_3^+ level at 1182 keV. In the present work, we concentrate on the study of the electromagnetic properties of the first two excited bands of ^{154}Gd, based on the 0_1^+ and 0_2^+ levels, in order to compare further observables to the predictions of the new X(5) critical point symmetry.

II. EXPERIMENT, DATA ANALYSIS AND RESULTS

The lifetimes of excited states in ^{154}Gd were measured using the recoil distance Doppler-shift (RDDS) method. The

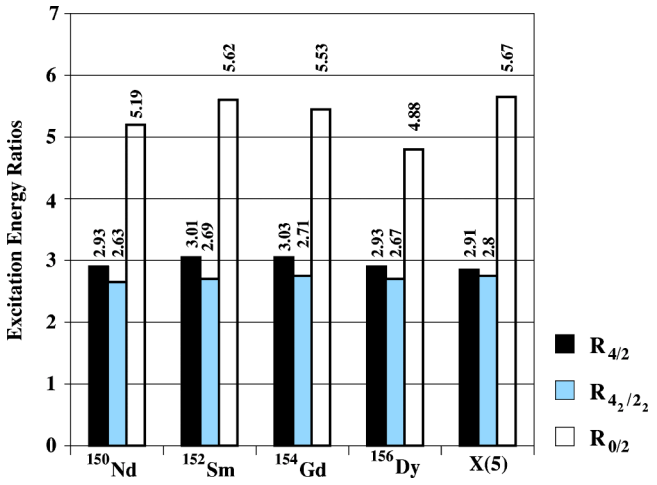

FIG. 1. (Color online) Comparison of the crucial experimental observables $R_{0/2}=E(0_2^+)/E(2_2^+), R_{4/2}=E(4_1^+)/E(2_1^+), R_{4_2/2_2}=(E_{4_2^+}-E_{0_2^+})/(E_{2_2^+}-E_{0_2^+})$ indicated on the ordinate for the $N=90$ rare earth isotones ^{150}Nd, ^{152}Sm, ^{154}Gd, and ^{156}Dy with the predictions of the X(5) dynamical symmetry. The isotones and X(5) are indicated on the abscissa. See also text.

*Present address: INFN, Laboratori Nazionali di Legnaro, Legnaro, Italy.

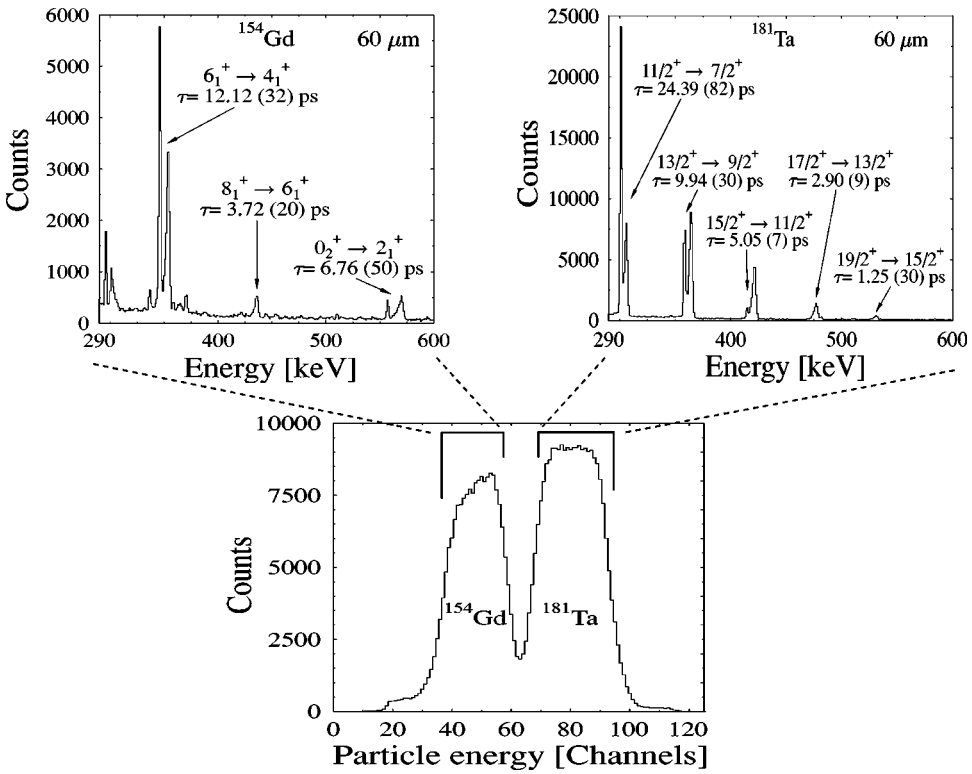

FIG. 2. Gates on the particle energies, corresponding to backscattered beam particles from the target and backing, and resulting γ-ray energy spectra of ^{154}Gd and ^{181}Ta at the target-to-stopper distance of 60 μm. For ^{154}Gd, shifted and unshifted components of the 347 keV $6_1^+ \rightarrow 4_1^+$ transition, the 427 keV $8_1^+ \rightarrow 6_1^+$ transition and the 588 keV $0_2^+ \rightarrow 2_1^+$ transition can be seen. Transitions and corresponding lifetimes are also labeled for ^{181}Ta. The spectra shown are measured with the cluster detector positioned at forward angle.

experiment was performed at the Cologne FN Tandem accelerator where a beam of ^{32}S with an energy of 110 MeV was used to Coulomb excite states in ^{154}Gd. The target consisted of 98% enriched ^{154}Gd isotope material evaporated to a thickness of 1 mg/cm^2 onto a 2 mg/cm^2 thick Ta foil. The recoiling nuclei left the target with a mean velocity v of 2.30(3)% of the velocity of light c and were stopped in a 5 mg/cm^2 Nb foil mounted together with the target in the Cologne coincidence plunger apparatus [10]. Data were collected for 23 target-to-stopper distances ranging from 1 to 2000 μm. The accuracy of the measurement of the relative target-to-stopper distances was better than 0.1 μm in the range from electrical contact to 20 μm and better than 1 μm in the range 20–200 μm.

The γ rays were detected with an Euroball cluster detector placed at 0° with respect to the beam axis, and four additional high efficiency germanium detectors positioned at the backward angle of 144°. This setup is very similar to the one reported in Ref. [11].

In order to fix the reaction kinematics, backscattered beam particles were detected by six photodiode cells, manufactured by SILICON SENSORS, which were mounted $\approx$1 cm upstream of the target to cover an angular range of 155°–175°. This range corresponds to target nuclei recoiling into a forward cone covering 0°–10°. By means of these photodiodes the ^{32}S nuclei backscattered from the Gd target or the Ta backing can be easily distinguished. This was essential to eliminate contaminations originating from the Coulomb excitation of the tantalum target backing.

The energy signals from the germanium detectors were recorded in coincidence with the energy signals from the particle detectors. The mean coincidence rate was about 2 kHz. As illustrated in Fig. 2, a proper gate on the particle energy allows us to distinguish the γ rays originating from ^{154}Gd and ^{181}Ta. (See also Fig. 2 caption.)

At each distance x, the lifetime is calculated according to the formalism of the differential decay-curve method (DDCM) in a "singles mode" presented in details in Ref. [12],

$$\tau(x) = -\frac{R_{ij}(x) - b_{ij}\dfrac{W_{ij}(\theta)\epsilon_{ij}}{(1+\alpha_{ij})}\displaystyle\sum_h R_{hi}(x)(1+\alpha_{hi})/W_{hi}(\theta)\epsilon_{hi}}{v \cdot \dfrac{d}{dx}R_{ij}(x)}. \tag{1}$$

Here, x is the target-to-stopper distance, $R_{ij}(x)$ is the area of the unshifted peak of the transition of interest, $t=x/v$ is the corresponding time of flight, b_{ij} is the branching ratio of the transition $i \rightarrow j$, and R_{hi} are the areas of the unshifted peaks of the direct feeding transitions. $W_{ln}(\theta)$ represents the angular distribution function for the transition $l \rightarrow n$ at the angle θ of observation with respect to the beam axis, α_{ln} is the internal conversion coefficient, and ϵ_{ln} is the efficiency of the germanium detector. We note that in our experiment, the angular distribution functions of the transition of interest and those of the feeding transitions are quite similar. An efficiency calibration of the germanium detectors was performed with a ^{152}Eu source.

Using Eq. (1) yields a set of lifetime values (the τ-curve) which should naturally lie on a straight line when plotted versus the distance x.

Compared to the intensity of the depopulating transitions, the observed feeding was less than 8 % in all cases due to the exponential drop of the Coulomb excitation strength at high

excitation energies. Since Coulomb excitation is highly selective for collective states, the possibility for unobserved feeding is negligible. In the final analysis, the observed feeding from above was taken into account.

Since the DDCM was applied to singles spectra and since Coulomb excitation in coincidence with backscattered particles produces highly oriented nuclear states, we investigated the possible impact of the nuclear deorientation effect. For each individual γ-ray transition employed in the lifetime determination, the constancy of the sum of the areas of in-flight and stop peaks was checked at all distances. Deviations from a constant behavior were found only for the 4_1^+ state. The investigation of the deorientation effect according to the approaches of Refs. [13,14] showed that this effect does not play a significant role in the case of the lifetime determination for the 4_1^+ state. The reason is that the data points used for this determination lie in a time region where the nucleus is already completely deoriented. This result is also supported by the fact that the lifetime of the 4_1^+ state determined in the present work in practice coincides with the values reported in earlier works [15,16] where Coulomb excitation was used. The 6_1^+ and 8_1^+ states are not significantly affected by the deorientation because of their high spins, the $0_2^+ \rightarrow 2_1^+$ transition has an isotropic distribution, and for the lifetime determination for the 2_2^+ and 4_2^+ states, only summed spectra from all seven cluster segments were analyzed. Thus, for the latter states, the angular distribution was integrated over a wide range and all effects related to it were averaged out.

The application of Eq. (1) for the lifetime determination of the 4_2^+ level is illustrated in Fig. 3 where the τ curve, the difference in the numerator and the derivative [denominator in Eq. (1)] are presented. This figure is also a demonstration of the quality of the data for the case of the weakest transition reported in this work. Lifetimes were derived from the data for the 4_1^+, 6_1^+, 8_1^+, 0_2^+, 2_2^+, and 4_2^+ levels in ^{154}Gd. The results are summarized in Table I. The quality of the experiment is demonstrated by the agreement within the error bars of the present results with literature values for levels with well-established lifetimes [15,16]. Small differences are observed for the lifetimes of the 6_1^+ (about 7%) and 0_2^+ (about 17%) states. The lifetimes determined in the present work are characterized by smaller uncertainties. The lifetime $\tau = 11.00(55)$ ps of the 4_2^+ level is determined for the first time. This lifetime is important since it doubles the number of absolute $B(E2)$ values now known involving the 0_2^+ band, giving several new interband transition probabilities and a second intraband $B(E2)$ value.

In our analysis, we use only the areas of unshifted peaks. In the case of the 4_2^+ level, only forward detectors were employed, since at the backward angle the unshifted peak was obscured by the shifted peak of the 692 keV transition. (See also Fig. 4). The values of the reduced transition probabilities $B(E2)$ derived from the lifetimes are presented in the Table I. In order to extract in-band transition quadrupole moments Q_t from these data, we employed the well-known formula

$$B(E2, I \rightarrow I-2) = \frac{5}{16\pi}\langle IK20|I-2K\rangle^2 (Q_t)^2 \qquad (2)$$

in which a value of $K=0$ was used.

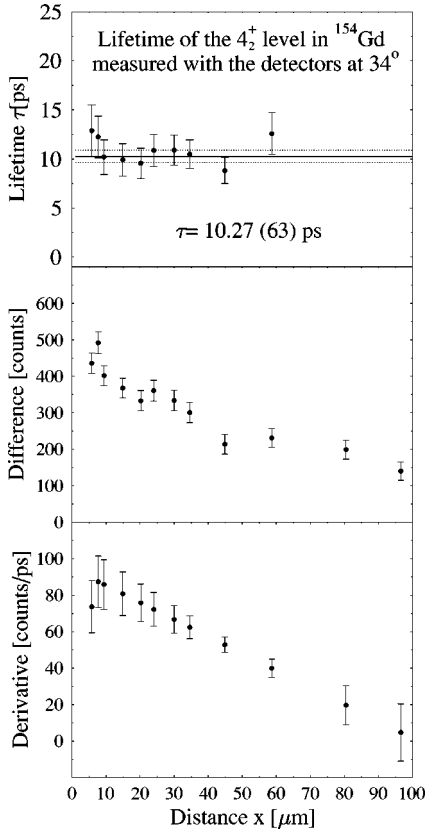

FIG. 3. Lifetime determination of the 4_2^+ level of the S2 band using data collected with the cluster segments positioned at 34°. The τ curve is presented in the top panel. It consists of lifetime values determined at different distances within the region of sensitivity. The mean value of the lifetime and its uncertainty are also shown. The distance dependence of the difference, which is the numerator on the right-hand side (rhs) of Eq. (1) is shown in the middle panel. The panel on bottom displays the derivative in the denominator on the rhs of the Eq. (1).

The lifetimes of excited states in ^{181}Ta, obtained as a by-product from the Coulomb excitation of the target backing, show an excellent agreement with the literature values. This fact also supports the reliability of the lifetimes derived in this work. Some lifetimes derived by us in ^{181}Ta are indicated in Fig. 2.

III. DISCUSSION

The $N=90$ nucleus ^{154}Gd is a direct even-even neighbor of ^{152}Sm which was the first nucleus where characteristic X(5) features were observed experimentally [19]. Since the energy spectrum of ^{154}Gd is very similar to that of ^{152}Sm [19] and also to that of ^{150}Nd [20], which was the second nucleus classified to be of X(5) type, it appears to be quite natural to test to what extent the X(5) predictions reproduce the experimental data for ^{154}Gd. It turns out that a classification based only on the excitation energies and branching ratios is not sufficient for a definite assignment as was shown in the case of ^{104}Mo. Bizzeti and Bizzeti-Sona [21] demonstrated that the energy spectrum of ^{104}Mo as well as relative

TABLE I. Analyzed transitions, derived lifetimes τ, and lifetimes reported in literature, experimental $B(E2)$ values, and X(5), GCM, and IBA theoretical predictions for the $B(E2)$ transition strengths. Branching ratios necessary for the derivation of the $B(E2)$ values were taken from NNDC [17]. Uncertainties of the experimental quantities are shown in brackets.

Transition	E_γ (keV)	$\tau_{this\ work}$ (ps)	$\tau_{literature}$ (ps)	$B(E2)_{exp}$ (W.u.)	$B(E2)_{X(5)}$ (W.u.)	$B(E2)_{GCM}$ (W.u.)	$B(E2)_{IBA}$ (W.u.)
$2_1^+ \rightarrow 0_1^+$	123		1708 (7) Ref.[18]	157.8 (6)	158	158	158
$4_1^+ \rightarrow 2_1^+$	248	65.5 (15)	64.9 (20) Ref.[17]	245.2 (58)	250	252	235
$6_1^+ \rightarrow 4_1^+$	347	12.12 (32)	11.25 (60) Ref.[17]	266 (7)	313	307	263
$8_1^+ \rightarrow 6_1^+$	427	3.72 (20)	3.69 (20) Ref.[17]	312 (17)	359	351	273
$0_2^+ \rightarrow 2_1^+$	558	6.76 (50)	5.77 (70) Ref.[17]	45.1(33)	100	85	52
$2_2^+ \rightarrow 0_2^+$	134	9.28 (50)	9.23 (50) Ref.[17]	54.0(36)	125	124	98
$\rightarrow 4_1^+$	444			20.0(11)	57	27	21.1
$\rightarrow 2_1^+$	692			6.3(4)	14	29	9.5
$\rightarrow 0_1^+$	815			0.9 (1)	3	0.4	0.33
$4_2^+ \rightarrow 2_2^+$	233	11.00 (55)		187 (13)	190	201	157
$\rightarrow 6_1^+$	330			14.2 (9)	44	22	14.9
$\rightarrow 4_1^+$	677			5.0 (5)	9	24	7.9
$\rightarrow 2_1^+$	925			0.54 (4)	1.54	0.02	0.25

transition probabilities can be nicely described by the X(5) calculations. Later, however, it was established by Hutter *et al.* [22] that the absolute $B(E2)$ values do not support an X(5)-like character of that nucleus.

As far as the energy spectrum of ^{154}Gd is concerned, the comparison with the X(5) predictions has already been performed in previous works (e.g., Refs. [23,24]). In Fig. 1, the crucial observables $R_{0/2}=E(0_2^+)/E(2_2^+), R_{4/2}=E(4_1^+)/(2_1^+)$, $R_{4_{2/2_2}}=(E_{4_2^+}-E_{0_2^+})/(E_{2_2^+}-E_{0_2^+})$ of the four $N=90$ isotones ^{150}Nd, ^{152}Sm, ^{154}Gd, and ^{156}Dy are compared to the corresponding X(5) values. As for ^{150}Nd and ^{152}Sm, for ^{154}Gd the agreement is also remarkably good.

The absolute $B(E2)$ values measured in this work allow now for a more stringent test of the X(5) predictions including excitation energies as well as relative and absolute transition probabilities.

Figure 5 shows the Q_t values within the gsb [band S1 according to the X(5) nomenclature] of ^{154}Gd together with the theoretical values of the X(5) symmetry, the symmetric rotor, and the IBA U(5) limit [25]. The four data sets are normalized to the experimental $Q_t(2_1^+ \rightarrow 0_1^+)$ value. The experimental transition quadrupole moment $Q_t(4_1^+ \rightarrow 2_1^+)$ agrees perfectly with the X(5) value. At higher spins, the experimental values lie between X(5) and the rotor values. The U(5) predictions are considerably higher for all states.

Of special importance are also the transition probabilities within the first excited band (S2) and those of the interband transitions between the S2 and S1 bands.

In Fig. 6, these quantities as well as the energy spectra of the S1 and S2 bands according to X(5) are compared to the corresponding experimental values in ^{154}Gd. Only two normalization factors, the excitation energy of the first 2^+ state and the $B(E2;2^+ \rightarrow 0^+)$, are used. The overall agreement is found to be good for both energies and transition probabilities, although as generally seems to occur, the absolute X(5) energy spacings in the S2 band are larger than observed, and the intraband $B(E2)$ values are also larger than measured.

As in the case of the $4_1^+ \rightarrow 2_1^+$ transition mentioned when the Q_t values in Fig. 5 were discussed, the $B(E2;4_2^+ \rightarrow 2_2^+)$ value is very close to the X(5) value. All other strong transitions are also well described, with the exceptions of $B(E2;2_2^+ \rightarrow 0_2^+)$ and $B(E2;0_2^+ \rightarrow 2_1^+)$, whose values are a factor of 2 smaller than the X(5) predictions. For the interband transitions, the measured strengths are found to be less than a factor of 2 smaller than the corresponding X(5) calculations which is similar to the case of ^{150}Nd [20]. In Ref. [20], this behavior is explained by the rapid change of many observables in the vicinity of the critical point of the phase transition. Therefore, small structural deviations from X(5) are amplified by these sensitive interband $B(E2)$ values. Noting that the yrast $B(E2)$ values are somewhat intermediate between the rotor and X(5), it is consistent that the experimental interband $B(E2)$ values tend in the same direction.

Summarizing, the agreement between the experimental data for ^{154}Gd and the X(5) predictions is found to be good and is comparable to the quality of agreement found for ^{150}Nd and ^{152}Sm. In all cases investigated so far perfect agreement with the X(5) predictions is of course, not observed. This is not surprising since the X(5) model does not employ any fitting and the underlying nuclear potential is approximated in a rather schematic way. That is, X(5) is not a model to be fit to the data as are models such as the IBA and GCM [26] but, rather, it is an invariant (except for scale) benchmark, similar in spirit to other idealizations such as the pure rotor or harmonic vibrator. In real nuclei those ideals are not reached and perturbations to them are necessary. Similarly, for X(5), the IBA and GCM allow for parametrized deviations from X(5).

Therefore one should expect an improved agreement between experimental and theoretical values when using other theoretical models where the calculated quantities can be ad-

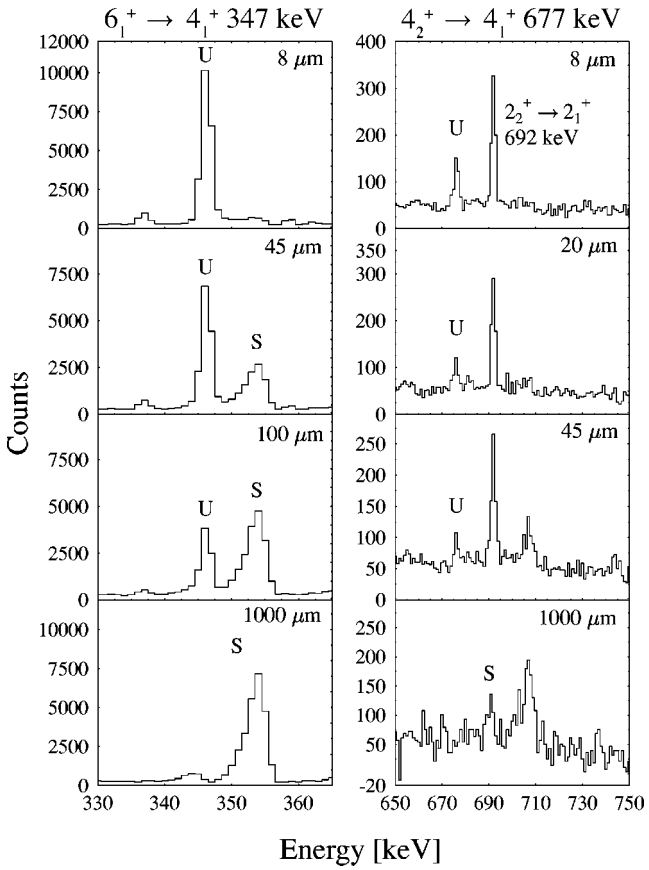

FIG. 4. Particle-gated γ-ray spectra of ^{154}Gd taken at four different distances. Summed spectra from all detectors at forward angles are shown. On the left-hand side, both shifted and unshifted peaks of the $6_1^+ \rightarrow 4_1^+$ transition are presented. On the rhs, the shifted and unshifted peaks of the $4_2^+ \rightarrow 4_1^+$ transition are shown. The obscuring transition of 692 keV ($2_2^+ \rightarrow 2_1^+$) is also indicated on the rhs. At the distance of 1000 μm, this transition is fully shifted to a higher energy and correspondingly the shifted peak of the $4_2^+ \rightarrow 4_1^+$ of 677 keV transition can be observed (denoted by S).

justed by varying model parameters, such as with the IBA, GCM, or the PPQ [27] models. Such a comparison has been discussed by Clark *et al.* [28] and in Ref. [29] for the case of ^{152}Sm.

In the case of ^{154}Gd, we tried to reproduce the experimental observables with optimized IBA and GCM calculations. The results are shown in Fig. 7. The IBA calculation with only two scaling and two fit parameters, ξ and χ, comes very

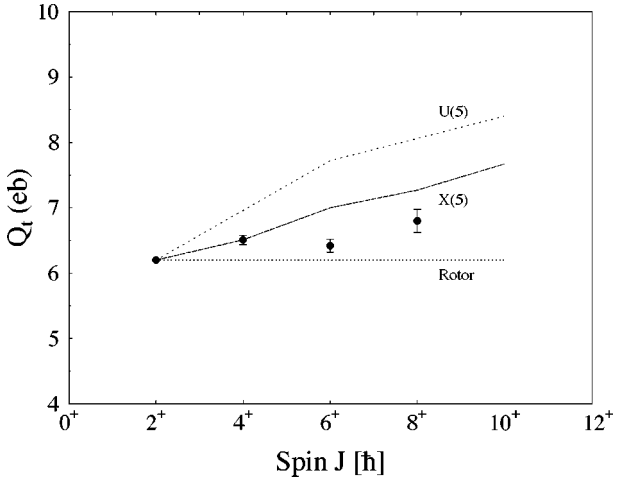

FIG. 5. Comparison of the Q_t values of the ground state band (band S1) in ^{154}Gd with the theoretical calculations of the X(5) dynamical symmetry, the symmetric rotor model and the U(5) limit of IBA. The data are normalized to the experimental $Q_t(2_1^+ \rightarrow 0_1^+)$ value. The lifetime of the 10^+ state necessary for derivation of the corresponding Q_t value was taken from the work of Sie *et al.* [16].

close to the experimental values including the sensitive S2 to S1 interband transition probabilities which are reproduced remarkably well. Also the GCM result can be considered to be satisfactory although six of the model parameters (in total eight) were employed in the calculation. The GCM Hamiltonian can be found in Ref. [26]. We used the parameters $B_2 = 49.1 \times 10^{-42}$ MeVs^2 and $P_3 = 0.0805 \times 10^{42}$ MeVs^2 for the kinetic energy terms, and $C_2 = -95.2$ MeV, $C_3 = 130.7$ MeV, $C_4 = 1261.5$ MeV, and $D_6 = 862.5$ MeV for the potential energy terms, respectively. As expected, the X(5) description is worse than those obtained with the IBA and the GCM since no fitting is involved.

Finally, we want to get some idea about the perturbation of the ideal X(5) model needed to describe ^{154}Gd. It was shown [30,31] that the critical point of phase transition between SU(3) and U(5) can be associated to the parameters $\xi = 0.026$ and $\chi = -\sqrt{7/4}$ of the IBA Hamiltonian given in that reference. The actual IBA fit shown in Fig. 7 was obtained with the parameter values $\xi = 0.028$ and $\chi = -\sqrt{7/4}$ which are very close to the critical point parameters. This leads to the conclusion that ^{154}Gd indeed can be located very close to the critical point of the SU(3)-U(5) phase transition for which the X(5) symmetry serves as a benchmark.

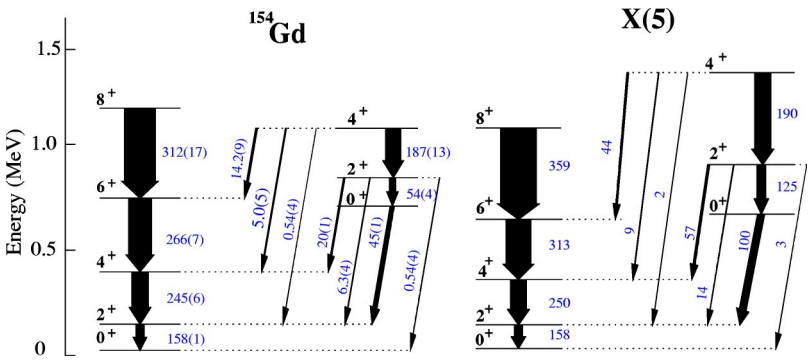

FIG. 6. (Color online) Comparison of the experimental level scheme of ^{154}Gd with the X(5) predictions. The $E(2_1^+)$ value (in keV) and the $B(E2; 2_1^+ \rightarrow 0_1^+)$ value (in W.u.) are normalized to the experimental data. The $B(E2)$ values are given next to the arrows.

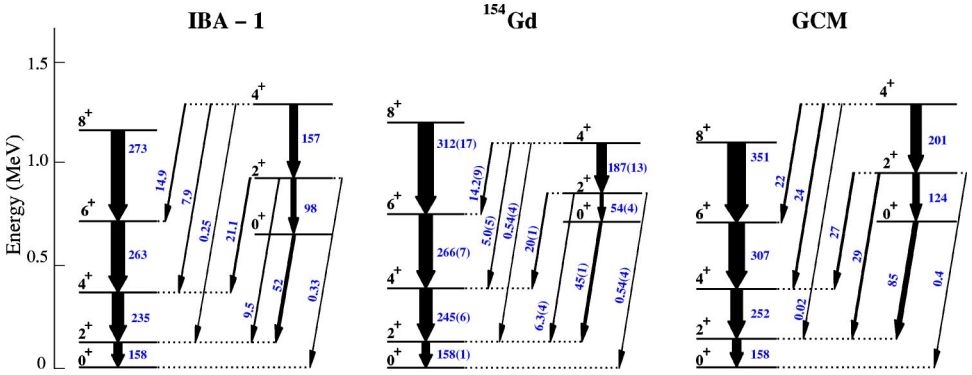

FIG. 7. (Color online) Comparison of the experimental level scheme of ^{154}Gd with calculations according to the GCM and IBA. As in Fig. 6, the model $E(2_1^+)$ value (in keV) and the $B(E2;2_1^+ \rightarrow 0_1^+)$ value (in W.u.) are normalized to the experimental data. The $B(E2)$ transition strengths are given next to the arrows.

IV. CONCLUSIONS

To conclude, RDDS lifetime measurements were carried out at the FN Tandem accelerator of the University of Cologne with Coulomb excitation of ^{154}Gd using a 110 MeV ^{32}S beam. From the derived lifetimes, 12 reduced $E2$ transition probabilities were determined whose values are in a good agreement with the predictions of the X(5) critical point symmetry as well with IBA and GCM calculations. The best result is obtained with a very simple IBA calculation showing that ^{154}Gd is situated at the SU(3)-U(5) phase transition very close to the critical point. Consistently, the different theoretical approaches show that ^{154}Gd can be associated with the critical point of a SU(3)-U(5) phase transition.

ACKNOWLEDGMENTS

D.T. expresses his gratitude to Ivanka Necheva for her outstanding support. Two of us (D.T. and P.P.) are grateful for the kind hospitality of the Cologne University. This work was funded by the BMBF under Contract No. 06 OK 167. This research has been financially supported by the European Community programme IHP under Contract No. HPMF-CT-2002-02018.

[1] F. Iachello, Phys. Rev. Lett. **85**, 3580 (2000).
[2] F. Iachello, Phys. Rev. Lett. **87**, 052502 (2001).
[3] A. Bohr and B. R. Mottelson, *Nuclear Structure* (Benjamin, New York, 1975).
[4] E. Nadjakov, R. Nojarov, and V. Antonova, Phys. Lett. **116B**, 207 (1982).
[5] C. Girit, W. D. Hamilton, and C. A. Kalfas, J. Phys. G **9**, 797 (1983).
[6] J. D. Morrison, J. Simpson, M. A. Riley, H. W. Cranmer-Gordon, P. D. Forsyth, D. Howe, and J. F. Sharpey-Schafer, J. Phys. G **15**, 1871 (1989).
[7] H. Tagziria, W. D. Hamilton, and K. Kumar, J. Phys. G **16**, 1837 (1990).
[8] S. Y. Chu, J. O. Rasmussen, M. A. Stoyer, P. Ring, and L. F. Canto, Phys. Rev. C **52**, 1407 (1995).
[9] W. D. Kulp. J. L. Wood, K. S. Krane, J. Loats, P. Schmelzenbach, C. J. Stapels, R.-M. Larimer, and E. B. Norman, Phys. Rev. Lett. **91**, 102501 (2003).
[10] A. Dewald, P. Sala, R. Wrzal, G. Böhm, D. Liebertz, G. Siems, R. Wirowski, K. O. Zell, A. Gelberg, P. von Brentano, P. Nolan, A. J. Kirwan, P. J. Bishop, R. Julin, A. Lampinen, and J. Hattula, Nucl. Phys. **A545**, 822 (1992).
[11] T. Klug, A. Dewald, V. Werner, P. von Brentano, and R. F. Casten, Phys. Lett. B **495**, 55 (2000).
[12] A. Dewald, S. Harisopoulos, and P. von Brentano, Z. Phys. A **334**, 163 (1989).
[13] A. E. Stuchbery, Nucl. Instrum. Methods Phys. Res. A **385**, 547 (1997).
[14] P. Petkov, A. Dewald, A. Gelberg, G. Böhm, P. Sala, P. von Brentano, and W. Andrejtscheff, Nucl. Phys. **A589**, 341 (1995).
[15] N. Rud, G. T. Ewan, A. Christy, D. Ward, R. L. Graham, and J. S. Geiger, Nucl. Phys. **A191**, 545 (1972).
[16] S. H. Sie, D. Ward, J. S. Geiger, R. L. Graham, and H. R. Andrews, Nucl. Phys. **A291**, 443 (1977).
[17] NNDC database, www.nndc.bnl.gov
[18] H. Mach and B. Fogelberg, Phys. Rev. C **51**, 509 (1995).
[19] R. F. Casten and N. V. Zamfir, Phys. Rev. Lett. **87**, 052503 (2001).
[20] R. Krücken *et al.*, Phys. Rev. Lett. **88**, 232501 (2002).
[21] P. G. Bizzeti and A. M. Bizzeti-Sona, Phys. Rev. C **66**, 031301(R) (2002).
[22] C. Hutter *et al.*, Phys. Rev. C **67**, 054315 (2003).
[23] M. A. Caprio *et al.*, Phys. Rev. C **66**, 054310 (2002).
[24] A. Dewald *et al.*, Eur. Phys. J. A (in press).
[25] F. Iachello and A. Arima, *The Interacting Boson Model* (Cambridge University Press, Cambridge, 1987).
[26] G. Gneuss and W. Greiner, Nucl. Phys. **A171**, 440 (1971).
[27] K. Kumar, Phys. Rev. Lett. **26**, 269 (1971).
[28] R. M. Clark, M. Cromaz, M. A. Deleplanque, R. M. Diamond, P. Fallon, A. Görgen, I. Y. Lee, A. O. Macchiavelli, F. S. Stephens, and D. Ward, Phys. Rev. C **67**, 041302(R) (2003).
[29] R. F. Casten, N. V. Zamfir, and R. Krücken, Phys. Rev. C **68**, 059801 (2003).
[30] F. Iachello, N. V. Zamfir, and R. F. Casten, Phys. Rev. Lett. **81**, 1191 (1998).
[31] R. F. Casten, D. Kusnezov, and N. V. Zamfir, Phys. Rev. Lett. **82**, 5000 (1999).